Manuscript Details

Manuscript number	JCOMB_2017_494
Title	Effect of age and level of damage on the autogenous healing of lime mortars
Article type	Full Length Article

Abstract

Natural hydraulic lime-based mortars are recommended for retrofitting operations in historical buildings, primarily because of their high chemical-physical and mechanical compatibility; moreover, because their autogenous and engineering self-healing capacities. This work proposes a methodology to quantify the autogenous self-healing in terms of recovery of the compression strength and ultrasonic pulse velocity in samples made of natural hydraulic lime mortars; specimens were pre-cracked at different ages (14 - 84 days) and levels of damage (70% of the compression strength in pre-peak regime; 90% of the compression strength in post-peak regime), and then cured under water up to 28 days. The capacity of healing after two loading/healing cycles has been also investigated. An interdisciplinary approach has been pursued characterising the mechanical aspects of the healing and the chemical nature of the products via SEM/EDS analyses. The results have provided useful indication about the dependence of the self-healing capacity on the aforementioned variables.

Keywords	autogenous self-healing, compressive strength, UPV, lime-based mortar
Manuscript region of origin	Europe

Corresponding Author	Cristina De Nardi
Order of Authors	Cristina De Nardi, Antonella Cecchi, Liberato Ferrara, Alvise Benedetti, Davide Cristofori
Suggested reviewers	Didier Snoeck, Virginie Wiktor, Lupita Sierra-Beltran, paola antonaci, Marta Roig Flores

Submission Files Included in this PDF

File Name [File Type]

Cover_letter.pdf [Cover Letter]

Effect of age_autogenous self-healing.docx [Manuscript File]

To view all the submission files, including those not included in the PDF, click on the manuscript title on your EVISE Homepage, then click 'Download zip file'.

Università Iuav di Venezia

DIPARTIMENTO DI
ARCHITETTURA COSTRUZIONE
CONSERVAZIONE

Head of Department: Antonella Cecchi

DACC
ex convento delle Terese
Dorso Duro, 2206
30123 Venezia

Cristina De Nardi
cristinadenardi@iuav.it

Venezia,13 Feb 2017

Composites part B

Subject: Submission paper Effect of age and level of damage on the autogenous healing of lime mortars by authors

C. De Nardi, A. Cecchi, L. Ferrara, A. Benedetti, D. Cristofori.

Dear editor,
please find the attached manuscript entitled “Effect of age and level of damage on the autogenous healing of lime mortars”, authored by C. De Nardi, A. Cecchi, L. Ferrara, A. Benedetti, D. Cristofori.
We are submitting it to be considered for the possible publication in Composites part B

This manuscript describes original work and is not under consideration by any other journal. All authors approved the manuscript and this submission.

Authors, active in the self-healing materials fields, have been recently published in a proceedings conference, non-indexed periodical; however the authors ensure that no data or results in the manuscript has been published before in any form.

In this paper, we report on dependency of autogenous self-healing capacity of lime-based mortars on different variables: age and level of damage.
An interdisciplinary approach has been pursued characterising the mechanical aspects of the healing and the chemical nature of the products via SEM/EDS analyses.

It is authors’ belief that only the analysis of the whole set of results, as presented in the manuscript we are submitting for publication, can allow a clear understanding of the autogenous healing phenomenon.

Thank you for receiving our manuscript and considering it for review. We appreciate your time and look forward to your response.

Yours sincerely
Cristina De Nardi

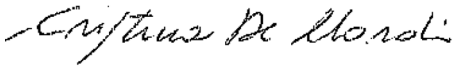

Effect of age and level of damage on the autogenous healing of lime mortars

C. De Nardi[1*], A. Cecchi[1], L. Ferrara[2], A. Benedetti[3], D. Cristofori[3]

[1] *Università IUAV di Venezia, DACC - Venezia, Italy*

[2]*Politecnico di Milano, DICA - Milano, Italy*

[3]*Università Cà Foscari Venezia, DSMN - Venezia, Italy*

Abstract

Natural hydraulic lime-based mortars are recommended for retrofitting operations in historical buildings, primarily because of their high chemical-physical and mechanical compatibility; moreover, because their autogenous and engineering self-healing capacities.

This work proposes a methodology to quantify the autogenous self-healing in terms of recovery of the compression strength and ultrasonic pulse velocity in samples made of natural hydraulic lime mortars; specimens were pre-cracked at different ages (14 - 84 days) and levels of damage (70% of the compression strength in pre-peak regime; 90% of the compression strength in post-peak regime), and then cured under water up to 28 days.

The capacity of healing after two loading/healing cycles has been also investigated.

An interdisciplinary approach has been pursued characterising the mechanical aspects of the healing and the chemical nature of the products via SEM/EDS analyses.

The results have provided useful indication about the dependence of the self-healing capacity on the aforementioned variables.

Keyword: autogenous self-healing, compressive strength, UPV, lime-based mortar

1. Introduction

Heritage buildings have been built with mud/clay bricks and lime-based mortars since quite early historical time, as confirmed by traces of ancient constructions in Palestine and Turkey dating back to 12.000 b. C. [1,2]

The reason for this long time use of lime as binder is its ability of accommodating movements and avoiding stress concentrations that can cause failure in brick masonry wall. In recent years, the use of lime-based mortars in restoration of cultural heritage has increased, also because of their chemical-physical and mechanical compatibility with old renders. In literature, several studies can be found regarding the compositions and properties of mortars for repairs, with an increasing interest in the use of pure lime and hydraulic lime mortars [3-5]. As a matter of fact, the incompatibility of the cement based mortars and ancient masonry has been clearly established due the presence of soluble salts, which can be dangerous for the original materials [6,7].

Lime mortar, instead, cannot be an efflorescence promoter, due to its relevant chemical purity [8]. Additionally, due to dissolution, transport and re-precipitation of calcium compounds, it can also have autogenous self-healing properties [9]. Despite the renewed interest in lime mortars for restoration purposes, researches have only seldom focused on their autogenous healing capacity as a benefit to the mechanical masonry behaviour.

Autogenous self-healing in lime-based mortars is an old well-known phenomenon, probably first recognized by Anderegg, [10] in 1942, who attributed this capacity, in mortars with high lime content, to the deposition of calcite in cracks. He also noticed that mortar made from hydrated dolomitic lime had a better performance than one high-calcium quicklime. [10].

Lubelli et al. [9], through microscopy analysis, highlighted that the presence of water, even in form of air moisture, is the necessary condition for the occurrence of self-healing. In fact, they observed that, in case of a relevant amount of free lime, water could be responsible of its dissolution and transport to the damaged area. Therefore, autogenous-healing is possible if atoms or molecules can

move from their initial position to the micro-crack surfaces, and there can re-crystallize to form calcium compounds. These processes of transport and re-precipitations of material (both $CaCO_3$ and $Ca(OH)_2$ have been observed) into voids and micro-cracks, are responsible for the reconstruction of the matrix trough-crack continuity and build-up of an enhanced load bearing capacity.

It is worth here remarking that a lot of studies in the last decade has been dedicated to the self-healing capacity of cement based materials [11,12] and several authors have investigated tailored additives or techniques purposely designed to enhance this capacity [13]. As a matter of fact the self-healing capacity depends on several factors, such as the mix composition of the matrix, the age of damage, the damage level, the external conditions (temperature, moisture) and the curing time [14].

With specific reference to lime-based mortars, the self-healing capacity has been regarded in most cases as a sort of bonus, occurred by coincidence or serendipity. Only in very recent years, a few studies have been dedicated to tailor the mortar composition to engineer the aforementioned capacity [15].

Nonetheless, the effects of this capacity on the recovery of mechanical properties and the influence on it of different experimental variables as the ones highlighted above have been rarely investigated.

In this work, a methodology is proposed to investigate the autogenous healing capacity of lime-based mortars through the recovery of compressive strength after pre-damaging specimens at different ages and levels of damage.

The effect of repeated damaging/healing cycles has been also taken into account with the aim of reproducing in the experiments – as close as possible – the conditions which mainly occur in real in-situ situations.

2. Materials

Four series of 50 mm sides cubes were made employing a lime-based mortars with the composition described in **Table 1**

Table 1. Mix design of investigated lime mortar

Constituent	Reference mortar
Slaked lime /dolomitic sand ratio*	1/3
Water /lime ratio (w/l)	0.22 l/kg
HHL5/ $Ca(OH)_2$ ratio	1/1

* aggregate standard UNI EN 1015-1.

The mix composition actually replicates as accurately as possible the one of lime mortars which can be found in heritage buildings, with the aim of likely use in retrofitting and restoration works [16, 17]. The chemical composition of the lime is summarized in **Table 2**

Tab 2: Chemical analysis of the main components of the limes, percentages related to original dry material.

Aggregate	CaO	MgO	Al_2O_3	K_2O	Na_2O	Fe_2O_3	SiO_2
NHL5	62%	1%	5%	0,7%	0,3%	3,5%	21%

The specimens were demoulded 96 hours after casting (during which time they stayed in a lab environment) and were then stored in a room at (23 ± 2)°C and (50 ± 4%) RH until the age of testing [18].

2.1 Microscopy observation on undamaged samples

In order to provide a deeper insight into the nature of the healing phenomena, the morphology, the crystal phases and the chemical composition of the investigated lime mortar and of its healing products were characterized by means of scanning electron microscopy (SEM) and X-ray diffraction (XRD).

The former was carried out with a Jeol JSM-5600 LV, a variable pressure instrument (VP-SEM) equipped with an Oxford Instruments Isis Series 300 energy dispersive x-ray spectroscopy (EDS) system. Samples were characterized mainly with no dedicated preparation procedure, exploiting the variable pressure capabilities of the instrument and using backscattered electrons (BSE) as the imaging signal. When needing higher resolution in order to find finer details, samples were coated

with a thin gold layer using a Polaron SC7620 sputter coater; in this case the secondary electron (SE) signal was used as the imaging signal.

X-ray powder diffraction (XRPD) spectra were recorded with a 170 Philips X'Pert powder diffractometer (Bragg−Brentano parafocusing geometry). A nickel-filtered Cu Kα1 radiation (λ = 0.15406 nm) and a step-by-step technique (step of 0.05° 2 h) with collection times of 10 s/step were employed.

Analyses were performed on virgin mortar samples tested for compressive strength at 28 day (no healing) and on fragments collected from cracked samples in mortar specimens pre-damaged at 56 days and kept 14 days in water.

As can be seen in **Fig 1**, mortar is made of grainy matrix, with pore size ranging from 2 to 500 μm, fine aggregates with irregular shape and size in the range of about 20-500 μm.

Fig 1: SEM images of undamaged mortar sample, 28 days age (a); EDS analysis of the surface of an aggregate, at point a (b); EDS analysis of the surface of mortar matrix, at point b (c)

The EDS analysis of the surface of the aggregate, reported in **Fig 1 (b)**, shows the presence of calcium, oxygen, magnesium, silicon and aluminum. The EDS analysis of the mortar matrix, in **Fig 1 (c)** highlights the presence of calcium, oxygen, magnesium, silicon, aluminium, potassium and sulphur. Both previous EDS micro-analysis are comparable with the chemical components of the binders and the dolomitic aggregates, as described above.

As can be seen in **Fig 2**, the presence of dolomite and calcium carbonate was confirmed by X-ray diffraction.

Fig 2: X-ray diffraction of mortar fragments

A further insight into the mortar composition can be got through analyses at higher magnification. As it can be seen in **Fig 3**, SEM analysis shows a longitudinal micro-crack (A). The EDS microanalysis were performed on the exposed surfaces of the micro-crack, at points a-b (**Fig 3 b**) and in the matrix

area at points c-d (**Fig 3c**). The comparison between these EDS spectra highlights that areas a-b – collected in the micro-crack – are richer in Mg but poorer in Si and Al than the points c-d – collected in the matrix. The presence of MgO and impurities such as silica, and alumina, especially inside of the crack edge, can promote the self-healing capacity of dolomitic mortars as demonstrates by recent studies of Lubelli [9].

Fig 3: SEM images of mortar along the crack surface (a); EDS at point a and b (b); EDS at point c and d (c). Different offset for each curve is plotted.

3. Methodology – mechanical and chemical characterization

In this work all specimens have been evaluated by means of uniaxial compressive tests, UPV (Ultrasonic Pulse Velocity) measurements and SEM (scanning electron microscopy) observations. As can be seen in **Fig 4**, the experimental programme consisted of four phases as hereafter described in detail.

In the first phase, the compressive strength of the mortar was determined at different ages (14, 28, 56 and 84 days):

- by testing three specimens at each age. Before testing, Ultrasonic Pulse velocity tests were performed on each specimen, according to the three x-y-z direction, as shown in **Fig 5**. The x direction has been henceforth assumed normal with the loading one.

Similarly, SEM and EDS analysis have been performed on fragments of the mortar matrix.

The UPV tests were performed by means of a portable equipment, composed by the source/detector unit and the surface transducers, which works in the frequency range of 10 Hz to 20 kHz; the passed time between input and output of the wave is measured with resolution of at least 0.01 μs.

Compressive strength tests were performed in displacement control using a Galdabini Sun 20 testing machine and at a displacement ratio equal to 0.2 mm/min.

Fig 4: scheme of experimental programme

Fig 5: scheme of UPV measurements along the three-xyz directions.

- at the same ages of testing other specimens were pre-damaged respectively at 70% of the compressive strength (measured as above) in the pre-peak regime and at 90% of the same strength in the post-peak regime.

Three specimens per each level of damage and age were pre-damaged employing the same methodology as in the compression strength tests discussed above.

Before and after pre-damaging, UPV measurements were taken for these specimens as well, always according to the procedure in **Fig 5**. Three damaged specimens per level, together with three further undamaged specimens per each pre-cracking age, were then cured in water for two different periods equal to 14 and 28 days.

- at the end of the curing periods as above, all specimens were re-analysed by means of UPV test end re-tested up to the maximum achievable compressive strength and then re-cured in water for further 14 days. After the aforementioned compressive tests, SEM and EDS analyses were performed on fragments of the mortar matrix. At the end of this second curing period, specimens were finally tested to failure (UPV measurements were taken once again before this first test).

The recovery, in case, of compressive strength along the cracking and healing cycles and the comparison with the normal aging and strength evolution of undamaged specimens will allow the effects of healing to be quantified and connected to the recovery of the damage level as through UPV tests [19].

4. Experimental results and discussion

4.1 Instantaneous compressive strength

In **Tab 3** the results of instantaneous monotonic compressive strength tests are shown for the different testing ages, together with results of UPV test measurements along the three xyz directions (x always normal to the loading direction and y/z perpendicular to it, as already seen in **Fig 5**).

Tab 3: Instantaneous monotonic compressive strength and UPV measurements

Loading age	Strength	UPV (m/s)		
days	(Mpa)	face x	face y	face z
14	2.09 (0.16)	1588	1640	1605
28	2.04 (0.17)	1539	1583	1504
56	1.61 (0.23)	1360	1413	1354
84	1.20 (0.06)	1272	1299	1266

The results shown are the average of three nominally identical specimens (in brackets, the standard deviation is also reported). It can be observed that the strength tends to decrease with time after 28 days. This is in line with the results obtained by Lanas et al (2006), who tested the strength development of lime mortars up to 182 days highlighting a not clear trend and attributing it to the occurrence of carbonation process [20].

In the case of the specimens herein tested – because of the quite dry atmosphere of the laboratory – some drying shrinkage phenomena may have also occurred, which likely justifies the measured compressive strength decrease. With reference to UPV measurements, they confirm the substantial isotropy of the undamaged specimens (measurements were taken before the test) and the expectable correlation (well know from the literature) with the compressive strength [21, 22]. In **Fig 6** the relation between UPV measurements and compressive strength is represented.

Fig 6: relation between UPV measurements and compressive strength; on face x - normal to load (a) and on face y - parallel to load – (b)

4.2 Pre-damage

At the aforementioned different ages (14, 28, 56 and 84 days), specimens were pre-damaged at two different levels, respectively equal to 70% of the compressive strength (as previously measured on a set of companion specimens) in the pre-peak regime and at 90% of the same aforementioned strength in the post-peak regime.

Immediately after damaging, UPV measurements were taken on the specimens.

The pre-loading at 70% of the compressive strength in the pre-peak regime did not result (as compared to the results on virgin specimen) into any significant damage, as can be seen in **Tab 4**.

Tab 4: UPV measurements after pre-loading at 70% of the compressive strength in pre-peak regime

Loading age	UPV (m/s)		
days	face x	face y	face z
14	1510	1589	1585
28	1513	1584	1469
56	1370	1432	1377
84	1214	1263	1245

On the other hand, a significant decrease of the ultrasonic pulse velocity can be observed for specimens pre-damaged beyond the peak and up to 90% of the compressive strength, as from **Tab 5**.

Tab 5: UPV measurements after pre-loading at 90% of the compressive strength in post-peak regime

Loading age	UPV (m/s)		
days	face x	face y	face z
14	1267	926	1018
28	1048	764	767
56	1063	823	852
84	969	762	795

A damage index D can be define as

$D = 1- v/v_0$

where v is UPV velocity after the pre-damage phase and v_0 is the UPV velocity of undamaged samples.

As it can be seen in **Tab 6**, the damage induced in pre-peak regime can be considered null, independently of the age of the samples and of the load direction. On the contrary, the damage in

post-peak regime, is affected by the load direction. As a matter of fact, in each series, micro-cracks created by the loading have determined a damage index parallel to the loading direction almost twice as high as normal to it.

Tab 6: Index of damage (D)

	70% pre-peak			90% post-peak		
Age (days)	face x	face y	face z	face x	face y	face z
14	-5%	-2%	-2%	21%	42%	36%
28	0%	1%	-2%	-30%	-51%	-49%
56	-1%	-1%	0%	-23%	-43%	-40%
84	-6%	-1%	-4%	-24%	-41%	-38%

4.3 First healing

As summarized in **Tab 7** and plotted in **Fig 7**, with reference to compression strength, the first step of the curing phase has highlighted the following results:

- comparing the compressive strength of undamaged samples, immersed in water for each curing period of 14 and 28 days, to the ones placed in lab environment, a significant improvement of the strength can be observed. As expectable, the aforementioned improvement decreases with the age of the sample. The compressive strength gain, observed by increasing from 14 to 28 the days of water immersion, also gradually decreases with the age of the samples to become insignificant (10-15% at earlier age).

- samples pre-damaged at 70 % of the compressive strength in pre-peak regime, show an interesting gain of the strength, quite similar to undamaged samples (differences are typically on the order of 5%). This is not surprising because the level of damage induced by preloading, as already observed, is very limited. The maximum gain, also in this case, is obtained in the first 14 days of curing time.

- samples pre-damaged at 90% of the compressive strength in post-peak regime, show an interesting healing capacity. The recovery of the compressive strength, after curing in water, is already of 20% after the first 14 days and it doubles after 28 days. Samples pre-damaged at 90% in post-peak regime, after 14 and 28 days curing in water, featured respectively a strength which is about 85% and 95% of the strength of companion undamaged specimens undergoing the same conditioning history. The gain

of compressive strength, observed by increasing from 14 to 28 the days of water immersion, gradually decreases with the age of the samples, as in previous cases. The relationship between healing capacity and age of samples is perfectly in line with other research work [23].

Tab 7: Experimental results of compressive strength after first healing cycle

Age (days)	Pre-damage loading	Compressive strength after 14 days in water (MPa)	Compressive strength after 28 days in water (MPa)
14	0%	3.11 (0.16)	3.40 (0.43)
14	70% pre-peak	2.99 (0.36)	3.32 (0.14)
14	90% post-peak	2.67 (0.29)	3.28 (0.34)
28	0%	2.57 (0.21)	2.75 (0.25)
28	70% pre-peak	2.54 (0.24)	2.78 (0.17)
28	90% post-peak	2.32 (0,15)	2.55 (0.16)
56	0%	2.15 (0.11)	2.43 (0.12)
56	70% pre-peak	2.00 (0.06)	2.69 (0.11)
56	90% post-peak	1.82 (0,04)	2.30 (0.40)
84	0%	1.61 (0.12)	1.55 (0.14)
84	70% pre-peak	1.53 (0.12)	1.44 (0.03)
84	90% post-peak	1.37 (0,03)	1.41 (0.05)

Fig 7: loss and recovery of UPV measurements after pre-peak (a) and post-peak (b) regime phase and after first healing cycle

Similarly, to the index of damage, with regards to the UPV measurements, an index of healing H can be calculated:

$H= (v_h-v_0)/v_0$

where, v_h is UPV velocity after healing curing time and v_0 is the UPV velocity of undamaged samples.

As from **Tab 8**, the UPV measurements confirmed the previous remarks. In detail:

- undamaged samples show a significant increase of UPV already after the first 14 days of curing time in water, except for the older sample (84 days); after 28 days the gain is almost double. Experimental data denoted a substantial isotropy.

- samples pre-damaged at 70% of the compressive strength in pre-peak regime, show a similar index of healing than the undamaged ones, both after 14 days and 28 in water. UPV measurements have confirmed the notes observed on the compressive strength values.

- samples pre-damaged at 90% of the compressive strength in post-peak regime, already after 14 days in water immersion featured a recovery of UPV almost of 10%, but only in earlier damaged samples. Significant differences can be observed along the three direction of the measurements. As expected the face x, which has had a lower damage, featured the best healing index. After 28 days of water immersion, all samples showed a performance quite comparable to the undamaged ones with the same conditioning history.

Tab 8: UPV measurements after first healing

Age (days)	Pre-damage loading	UPV after 14 days in water (m/s)			UPV after 28 days in water (m/s)		
		face x	face y	face z	face x	face y	face z
14	0%	1799	1886	1849	1976	2025	2029
14	70% pre-peak	1737	1835	1784	1937	2039	2040
14	90% post-peak	1756	1716	1605	1863	1917	1783
28	0%	1719	1721	1685	1885	1958	1889
28	70% pre-peak	1669	1702	1625	1873	1923	1882
28	90% post-peak	1605	1528	1476	1870	1786	1735
56	0%	1602	1610	1567	1664	1705	1680
56	70% pre-peak	1516	1566	1512	1715	1830	1748
56	90% post-peak	1445	1286	1297	1692	1434	1515
84	0%	1388	1395	1360	1347	1337	1386
84	70% pre-peak	1345	1338	1368	1349	1362	1341
84	90% post-peak	1286	1113	1132	1358	1335	1234

The relationship between compressive strength and UPV measurements is the same both in undamaged specimens and in damaged ones placed in water. Experimental results clearly show that the healing mechanism and the hydration is very similar (**Fig 8-9**)

Fig 8: undamaged samples, relationship between compressive strength and UPV velocity, after first healing; on face x normal to the load (a); on face y parallel to the load (b)

Fig 9: samples after post-peak regime pre-cracking phase, relationship between compressive strength and UPV velocity, after first healing; on face x normal to the load (a); on face y parallel to the load (b)

4.3.1 Microscopic observation on sample after healing phase

SEM /EDS analyses were also performed on fragments collected from a mortar sample 56 days aged, after the pre-cracking phase and the first curing time in water (**Fig 10**)

In every region of the mortar matrix very fine fibrous products are present. These microstructures were commonly found in self-healed cementitious matrix, as documented by a recent study of Gagné et al. [24]. EDS analysis (Fig 17) of the fibrous products in Fig 16 shows mainly the typical elements of hydration compounds of the lime-based mortar (calcium, oxygen and silicon in major amounts, in addition to magnesium, aluminium and potassium), a low peak of sulphur is also present.

Fig 10: SEM image of mortar samples, 56 days age after the pre-cracking phase and the first 28 days healing curing period (a); EDS analysis: the sample was sputter coated with gold, whose peaks are visible in the spectrum but not labeled because they do not belong to the sample (b)

4.4 Second cycle of healing

After the first healing cycle and the compressive tests performed to failure, all the samples did not disgregate and could be further handled. They were hence placed in water for a second healing cycle and were tested after 28 days of curing. All the results of this further testing stage are given in **Fig 11**; experimental data allow the following remarks to be highlighted:

- samples undamaged and pre-damaged at 70% of the compressive strength in pre-peak regime with the same history have the same compressive strength behaviour. The compressive strength are comparable and the period of first healing (14 days or 28 days) does not affect the final values.
- samples pre-damaged at 90% of the compressive strength in post-peak regime, in case of first healing of 14 days, feature compressive strength values 20% lower than the undamaged samples or the samples pre-damaged at 70% in pre-peak regime (3.59 vs. 2.86; 2.69 vs. 2.4). Otherwise, in the case of 28 days of first healing, samples feature a significant recovery of the compressive strength and show values really similar to the healthy samples undergoing the same history.

In **Fig 12** the comparison between the compressive strength, after the first healing and the second healing period is presented. The second time of curing phase has highlighted the following results:

- undamaged samples, show an increase of the compressive strength of about 10%, only in case of first healing of 14 days.
- samples pre-damaged at 70% in pre-peak regime, show an interesting compressive strength gain of about 20% in earlier samples damaged and in case of first healing of 14 days. After 28 days of first healing, the aforementioned gain reduced to half.
- samples pre-damaged at 90% in post-peak regime, show a compressive strength gain of 5%, which is always maintained. Data results clearly denote that the second healing determine not only a recovery of the compressive strength, but also an interesting gain of the mechanical properties.

Fig 11: variation in compressive strength after pre-damage, first healing, second healing. Undamaged samples (a); samples after pre-peak regime damage; samples after post-peak regime damage (c)

Fig 12: recovery of compressive strength after first healing cycle and second healing cycle.

5. Conclusions

In this study, a methodology has been proposed to measure the autogenous self-healing of lime mortars in terms of recovery of compression strength and ultrasonic pulse velocity (UPV). Samples were pre-cracked at different ages and at different levels of damage and cured under water for different times, including in case a repeated healing cycle.

Pre-damage phase is necessary to create micro-cracks, through which water can enter into the matrix to re-crystallize calcium compounds, which are thus able to fill and bridge the micro-cracks surfaces. Depending on the level of damage and on the age of pre-damage, natural hydraulic lime, even if added with calcium hydroxide, shows a relevant autogenous self-healing. From the analysed data, the following concluding remarks can be presented:

- already after 14 days in water immersion, samples damaged at 70% of the compressive strength in the pre-peak regime exhibit a recovery of the strength similar to the one featured by companion undamaged samples undergoing the same curing regime.

The strength increase with respect to the one measured at pre-cracking age, ranged from 40% to 25%, depending on the age of pre-cracking, being higher for earlier pre-damage age

- specimens pre-damaged at 90% of the compressive strength in the post-peak regime also exhibited a remarkable strength recovery, though lower than the previous case and always decreasing with the age of pre-cracking.

- increasing the curing time in water finally results into a further recovery of the strength but always decreasing with the age of pre-cracking. It can be reasonably assumed that after a well-timed curing phase, not only micro-cracks relating to an internal damage (as in case of pre-peak loading), but macro-cracks and fissures caused by a stress over the material failure, can be healed. Furthermore, the more moisture flow into the matrix, the better is the ability of healing agents (free lime) to be mobile over longer distances in order to fill the local damage spots.

- the correlation between the UPV and the compressive strength (and between the recovery of UPV and strength) follows the same trendlines and with equal reliability this confirm, for virgin and damaged samples, that the mechanism responsible of self-healing are the same of prolonged/continued hydration.

- after a second healing cycle, damaged specimens continued to exhibit a "residual" healing capacity (higher for less damaged specimens and pre-cracked at earlier ages) and even in case of post-peak regime damage, a compressive strength gain can be observed.

Acknowledgements

The authors wish to thank the technicians of the Construction/Materials Science Laboratory (Labsco), University Iuav, for their support in performing the experimental tests.

The authors also thank the technician Tiziano Finotto for the support in performing x-ray diffraction

analysis.

Conflict of Interest: the authors declare that they have no conflict of interest.

References

[1] Kingery WE, Introduction: some aspects of the history of ceramic processing in ultrastructure. In: Mackenzie, Ulrich, editors. Processing of advanced ceramics. New York: John Wiley; 1988. p. 1–29.

[2] von Landsberg D, The history of lime production and use from early times to the industrial revolution. Zement-Kalk-Gips,1992; 45: 199-203.

[3] Maurenbrecher, A.H.P, Mortars for repair of traditional masonry. In: Practice Periodical on Structural Design and Construction, 2004; 9(2): 62-65.

[4] Moropoulou A , Bakolas A, Moundoulas P., Aggelakopoulou E, Anagnostopoulou S, Strength development and lime reaction in mortars for repairing historic masonries. Cement & Concrete Composites; 2005; 27: 289–294. http://dx.doi.org/10.1016/j.cemconcomp.2004.02.017

[5] Lanas J, Alvarez G (2003), Masonry repair lime-based mortars: factors affecting the mechanical behaviour. Cement and Concrete Research, 2003; 33(1): 1867-1876. http://dx.doi.org/10.1016/S0008-8846(03)00210-2

[6] Moropoulou A, Polikreti, K, Ruf V, Deodatis G, San Francisco Monastery, Quito, Equador: characterisation of building materials, damage assessment and conservation considerations, Journal of Cultural Heritage, 2003;4:101-108 doi: 10.1016/S1296-2074(03)00021-9

[7] Veiga M.r, Aguiar J, Santos Silva A. Carvalho F, Methodologies for characterisation and repair of mortars of ancient buildings. In: Historical Constructions, P. Roca (Eds.), Guimarães, 2001, p 353-362

[8] Specification for Lime and its Uses in Plastering, Stucco, National Lime Association, Unit Masonry and Concrete, Washington DC (1966). http://anfacal.org/media/Biblioteca_Digital/Construccion/Mezclas_Repellados_y_Stuccos/Usos_de_la_cal_en_albanileria.pdf . accessed 10 November 2016

[9] Lubelli B, Nijland TG, van Hees RPJ, Self-healing of lime-based mortars: microscopy observations on case studies. 13th Euroseminar on Microscopy Applied to Building Materials; Ljubljana, Slovenia, 2011.

[10] Anderegg, F.O. (1942). Autogeneous healing in mortars containing lime, ASTM Bulletin,1942, 16:22.

[11] Van deer Zwaag S. Self Healing Materials, an Alternative Approach to 20 Centuries of Materials Science, Springer Series in Materials Science, 2007. doi:10.1007/978-1-4020-6250-6

[12] Van deer Zwaag S, Routes and mechanisms towards self healing behaviour in engineering materials. Bulletin of the polish academy of sciences Technical sciences, 2010; 58(2): 227–236 doi: https://doi.org/10.2478/v10175-010-0022-6, December 2010

[13] de Rooij M, Van Tittelboom K, De Belie N, Schlangen E, Self-healing Phenomena in Cement-Based Materials, State-of-the-Art Report of RILEM Technical Committee 221-SHC: Self-Healing Phenomena in Cement-Based Materials. 2012**.** ISBN 978-94-007-6624-2

[14] Nataliya Hearn, Self-sealing, autogenous healing and continued hydration: What is the difference? Materials and Structures/Materiaux et Constructions, 1998; 31:563-567 doi: 10.1007/BF02481539

[15] De Nardi C, Bullo S, Ferrara L, Ronchin L, Vavasori A, Effectiveness of crystalline admixtures and lime/cement microcapsules in engineered self-healing capacity of lime mortars, submitted Materials and Structures, 16 Gennaio 2017

[16] Penas F.E, Hydraulic lime mortars for wall rendering, Universidade Tecnica de Lisboa, 2008. httpps://Fenix.tecnico.ulisboa.pt. accessed 10 November 2016

[17] Silva, B A, Ferreira Pinto AP, Gomes A, Influence of natural hydraulic lime content on the properties of aerial lime-based mortars, Construction and Building Materials; 2014, 72: 208–218 doi: 10.1016/j.conbuildmat.2014.09.010

[18] WSDOT, Test Method T 813, Field Method of Fabrication of 2 in (50 mm) Cube Specimens for Compressive Strength Testing of Grouts and Mortars. 2015. http://www.wsdot.wa.gov/publications/manuals/fulltext/.../t813.pdf. accessed 10 November 2016

[19] W. Zhong, W. Yao (2008), Influence of damage degree on self-healing of concrete, Construction and Building Materials; 2008, 22: 1137-1142 doi:10.1016/j.conbuildmat.2007.02.006

[20] Lanas J. et al (2006), Mechanical properties of masonry repair dolomitic lime-based mortars, Cement and Concrete Research; 2006, 36 (5): 951-960. http://dadun.unav.edu/bitstream/10171/27764/1/2006-05-CEMCONRES.pdf accessed 10 November 2016

[21] Naik T. R, Malhotra V.M, Popovics J. S. The Ultrasonic Pulse Velocity Method. In: Handbook of Nondestructive testing of concrete. 2nd edn. CRC Press. 2004.

[22] Suaris W, Fernado V, Ultrasonic pulse attenuation as a measure of damage growth cyclic loading of concrete. ACI Mater, 1987, 84(3):185–93

[23] Ter Heide N, and Schlangen E, Self-healing of early age cracks in concrete, In: Proceedings of the First International Conference on Self Healing Materials 18-20 April 2007, Noordwijk aan Zee, The Netherlands, 2007

[24] R. Gagne´ R , Argouges M, A study of the natural self-healing of mortars using air-flow measurements, Materials and Structures; 2012, 45:1625–1638 doi:10.1617/s11527-012-9861-y

Figures

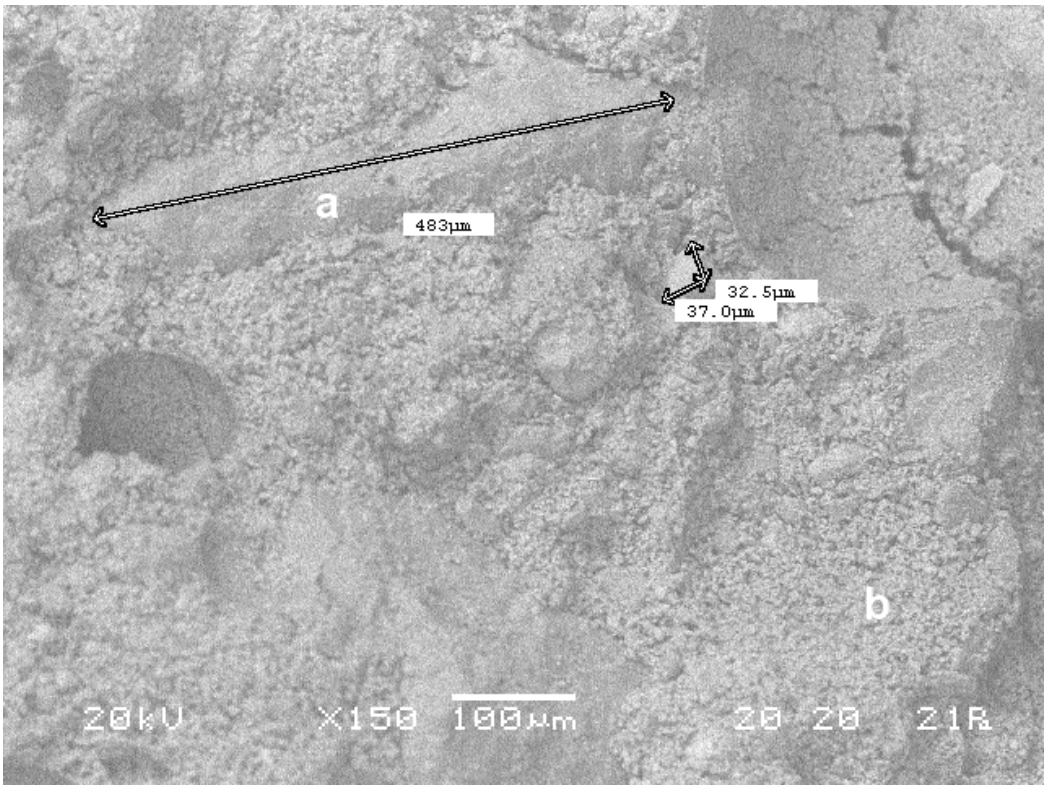
a
483µm
32.5µm
37.0µm
b
20kV X150 100µm 20 20 21R

(a)

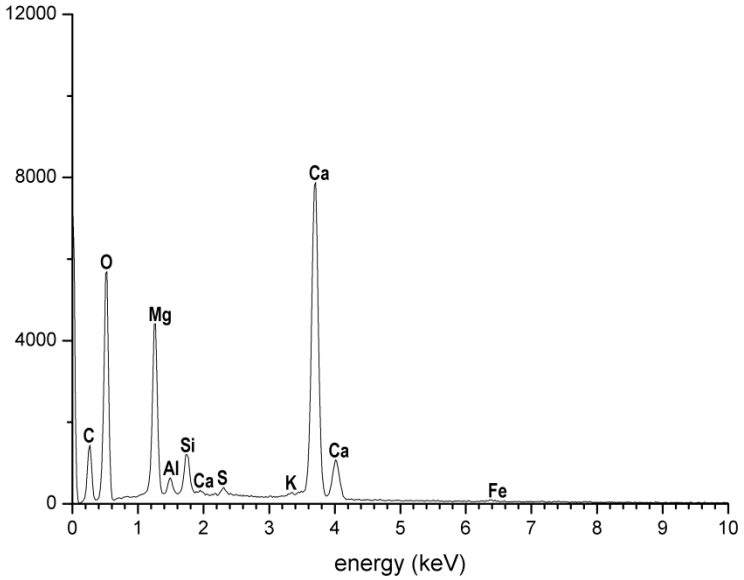
12000
8000
4000
0
C
O
Mg
Al
Si
Ca
S
K
Ca
Ca
Fe
0 1 2 3 4 5 6 7 8 9 10
energy (keV)

(b)

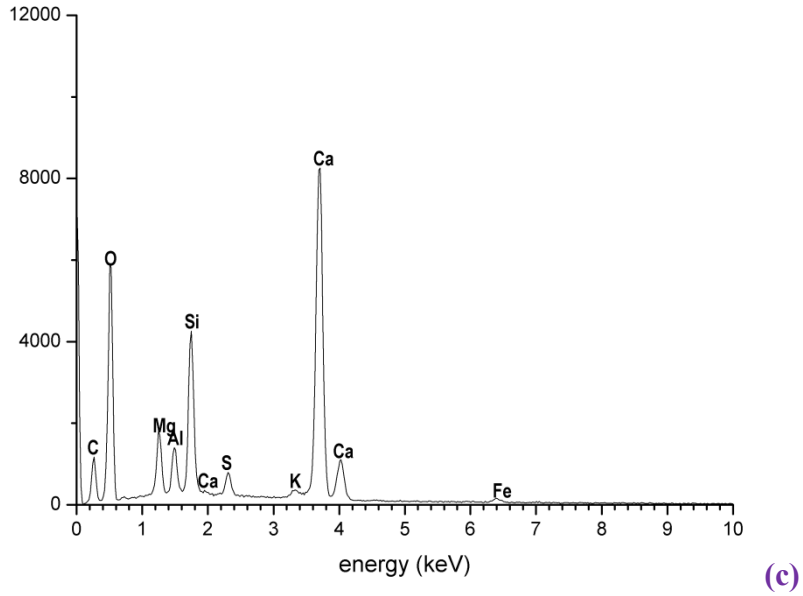

Fig 1: SEM images of undamaged mortar sample, 28 days age (a); EDS analysis of the surface of an aggregate, at point a (b); EDS analysis of the surface of mortar matrix, at point b (c)

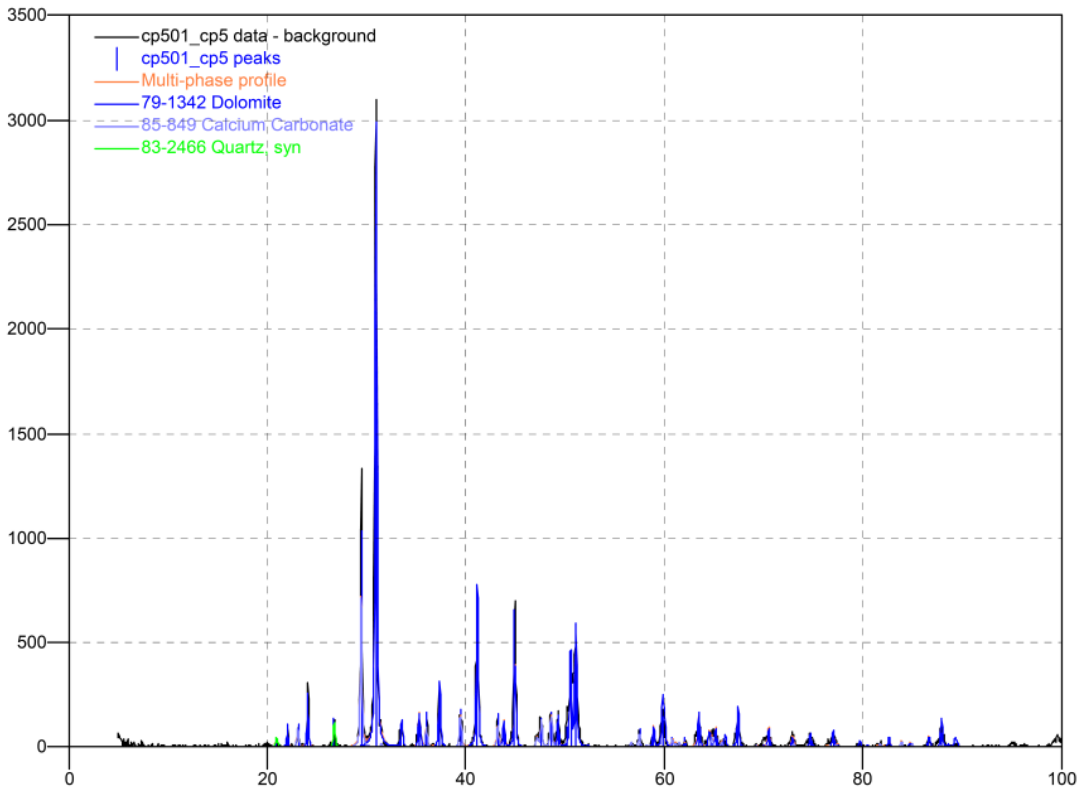

Fig 2: X-ray diffraction of mortar fragments

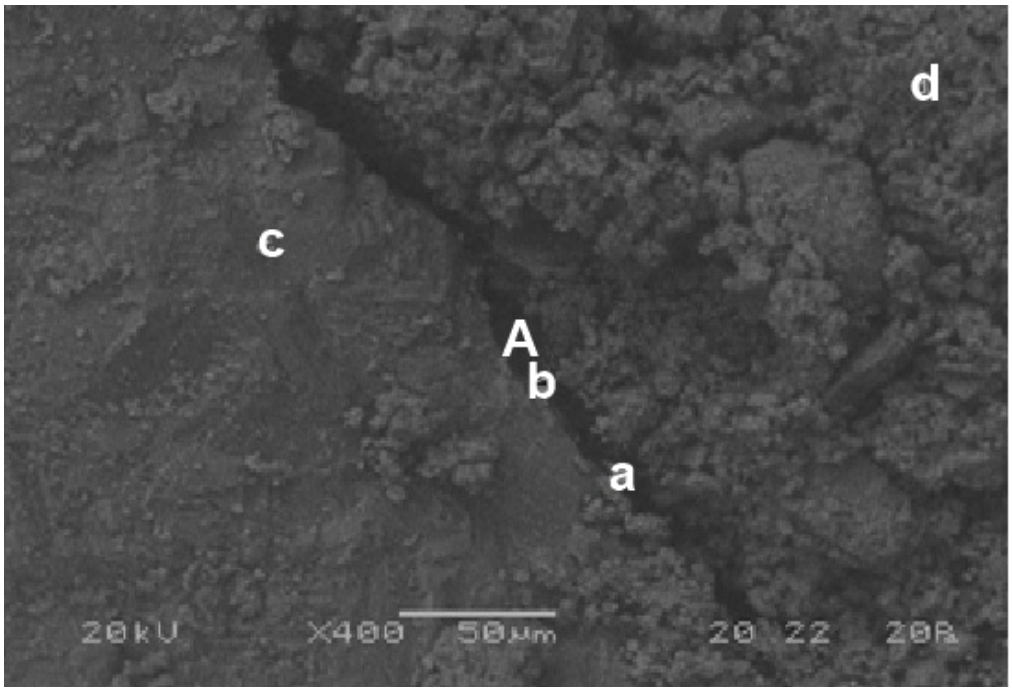
d
c
A
b
a
20kV X400 50µm 20 22 20R

(a)

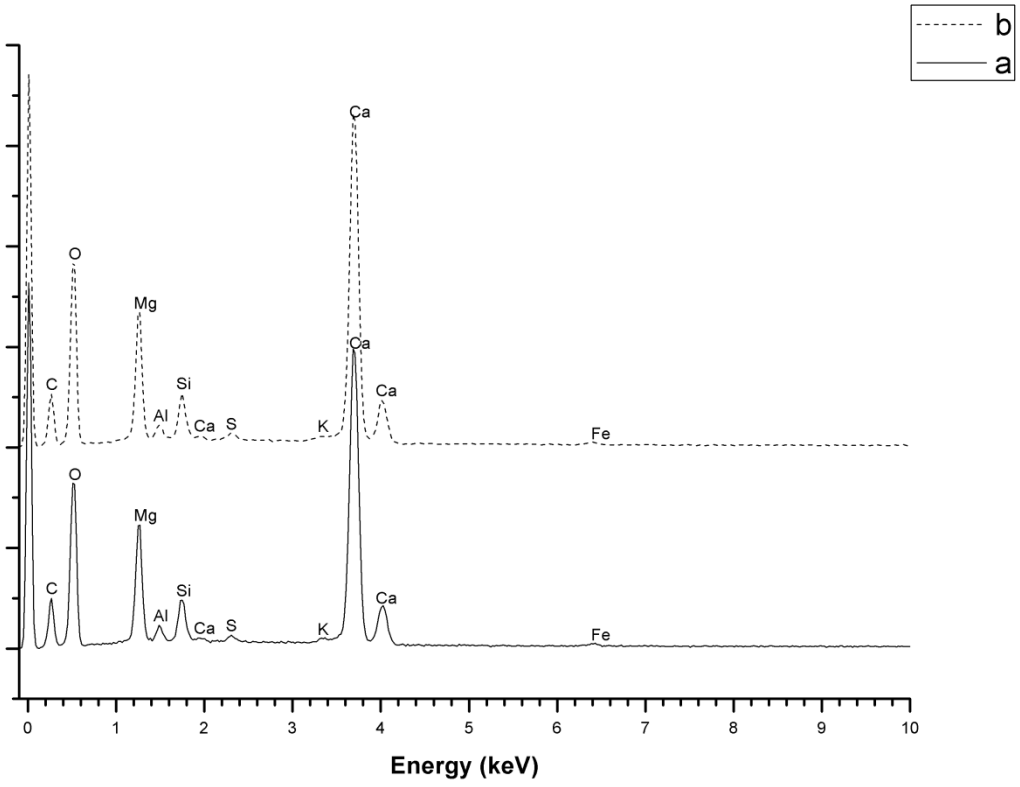
b
a
Ca
O
Mg
C
Si
Al
Ca
S
K
Ca
Ca
Fe
O
Mg
C
Si
Al
Ca
S
K
Ca
Fe
0
1
2
3
4
5
6
7
8
9
10
Energy (keV)

(b)

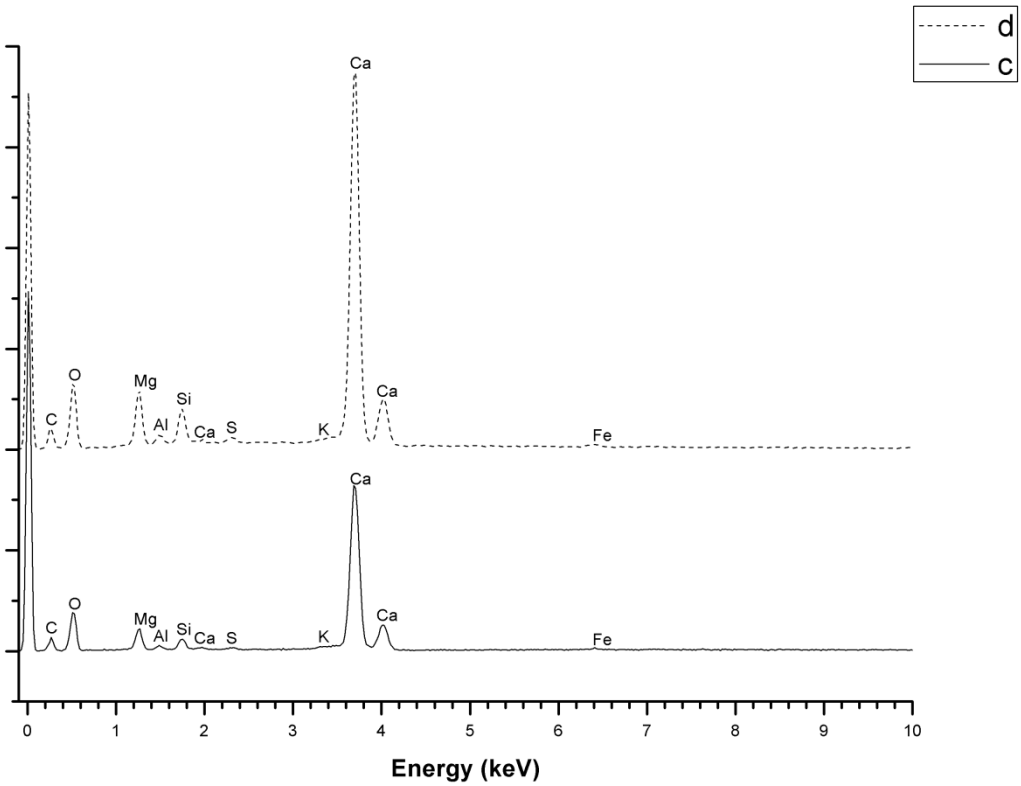

(c)

Fig 3: SEM images of mortar along the crack surface (a); EDS at point a and b (b); EDS at point c and d (c). Different offset for each curve is plotted.

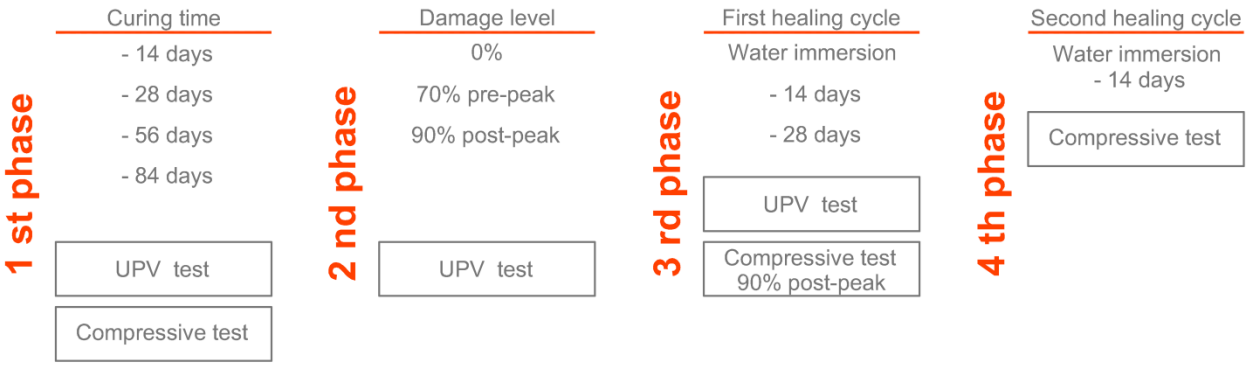

Fig 4: scheme of experimental programme

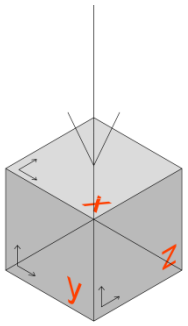

Fig 5: scheme of UPV measurements along the three-xyz directions.

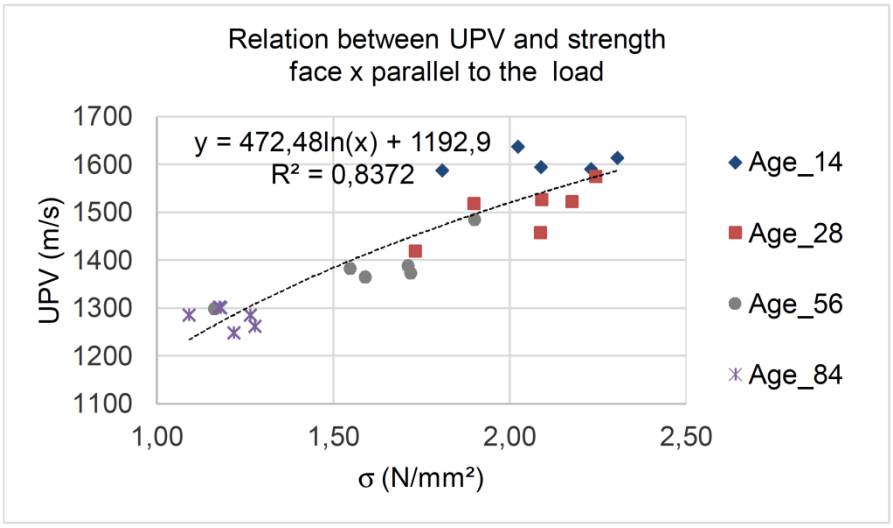

(a)

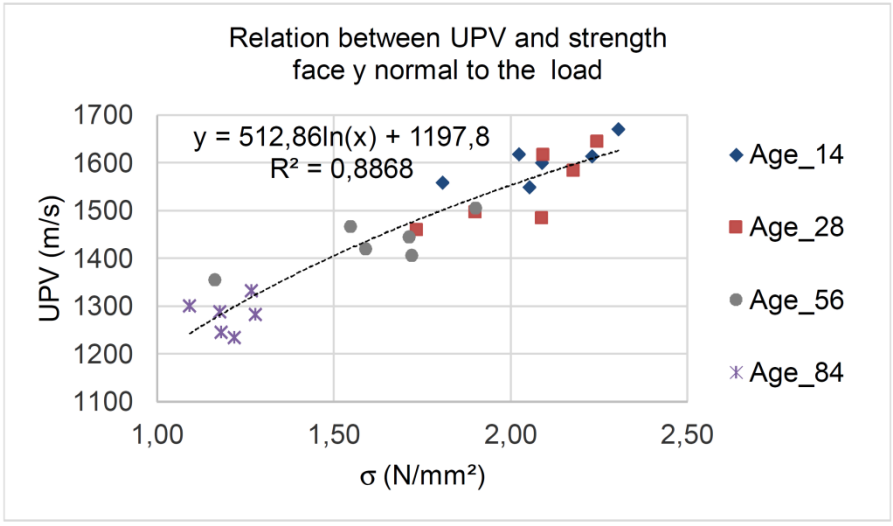

(b)

Fig 6: relation between UPV measurements and compressive strength; on face x - normal to load (a) and on face y - parallel to load – (b)

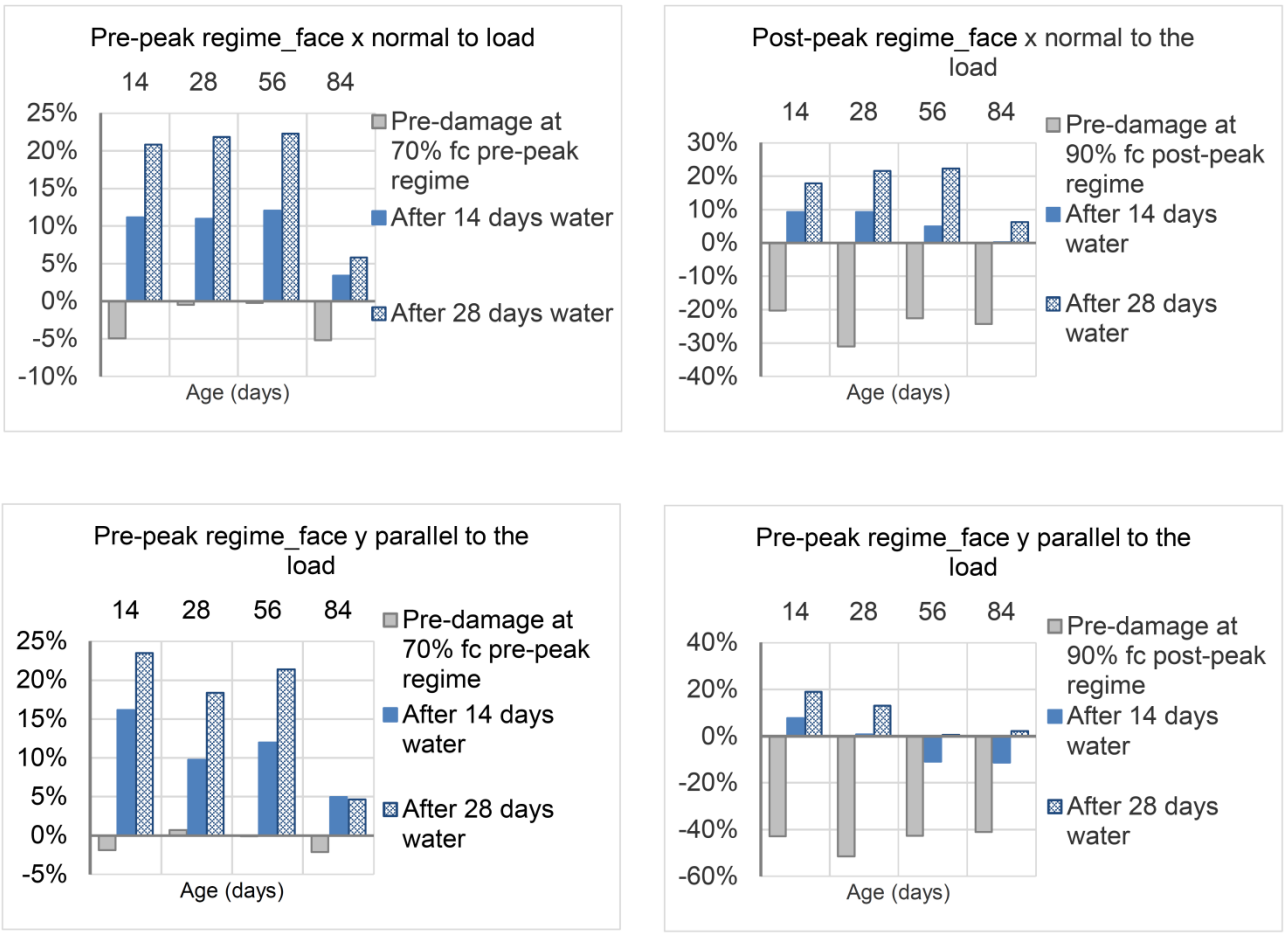

(a) (b)

Fig 7: loss and recovery of UPV measurements after pre-peak (a) and post-peak (b) regime phase and after first healing cycle

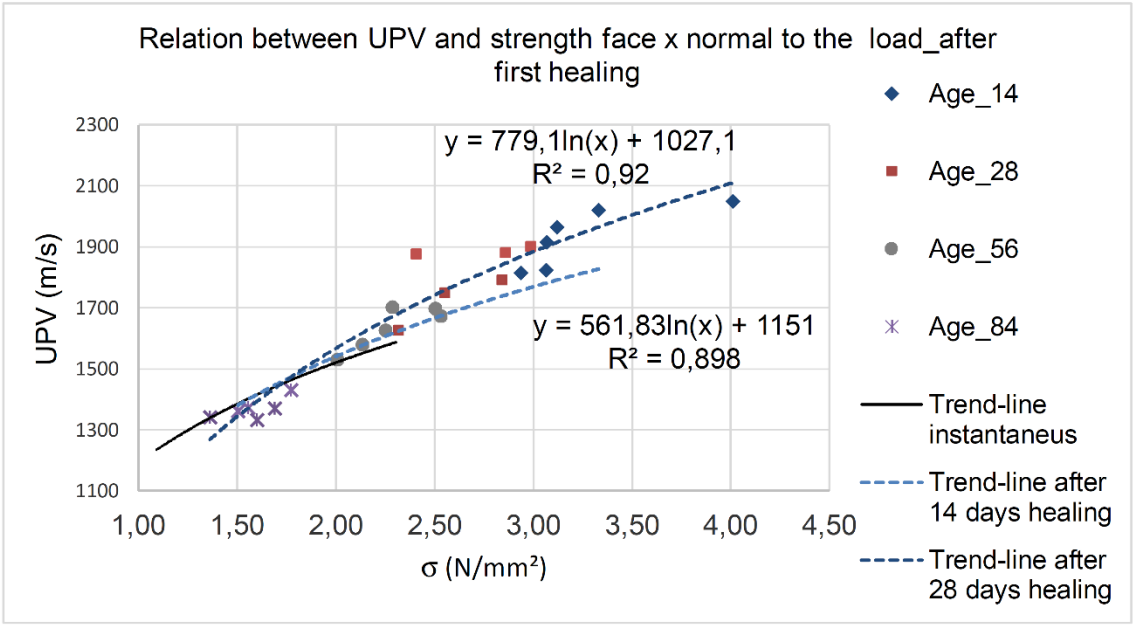

(a)

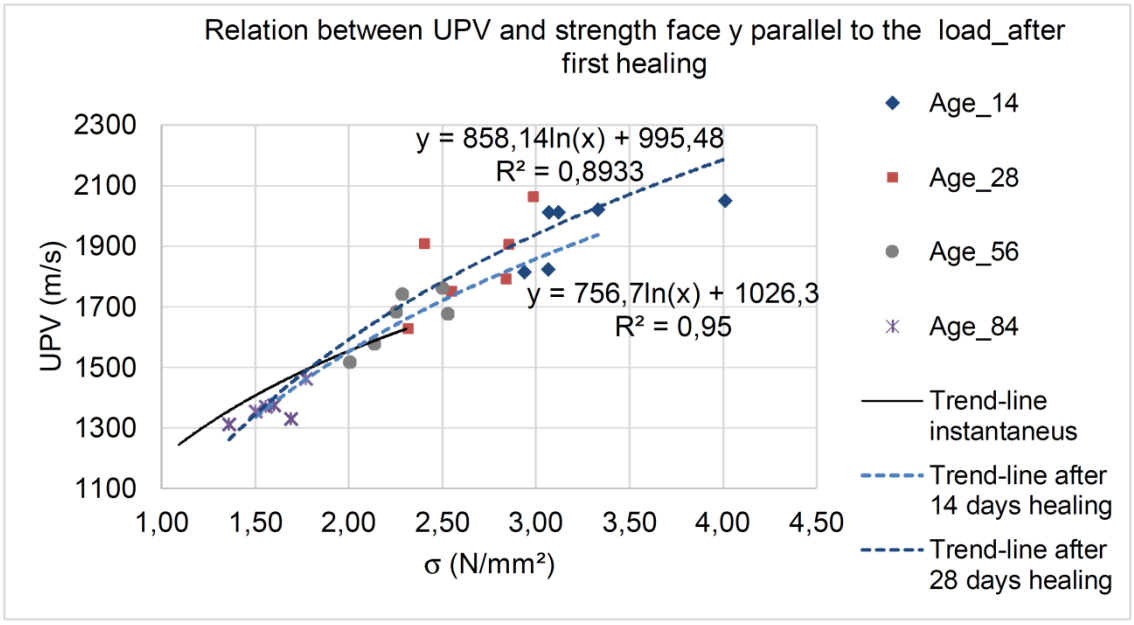

(b)

Fig 8: undamaged samples, relationship between compressive strength and UPV velocity, after first healing; on face x normal to the load (a); on face y parallel to the load (b)

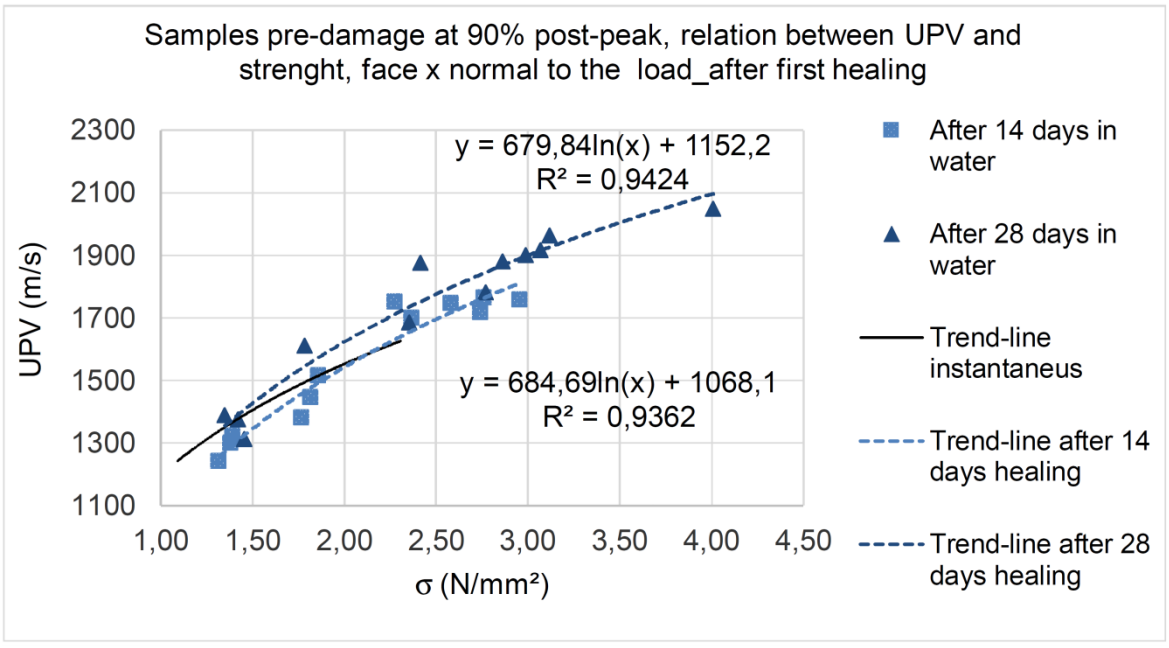

(a)

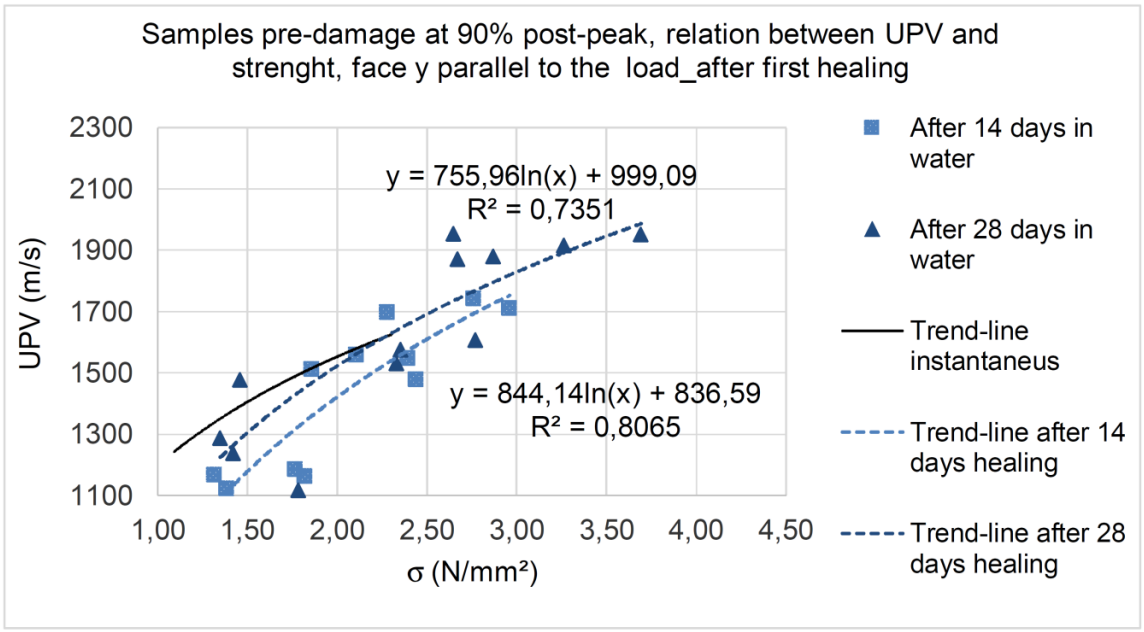

(b)

Fig 9: samples after post-peak regime pre-cracking phase, relationship between compressive strength and UPV velocity, after first healing; on face x normal to the load (a); on face y parallel to the load (b)

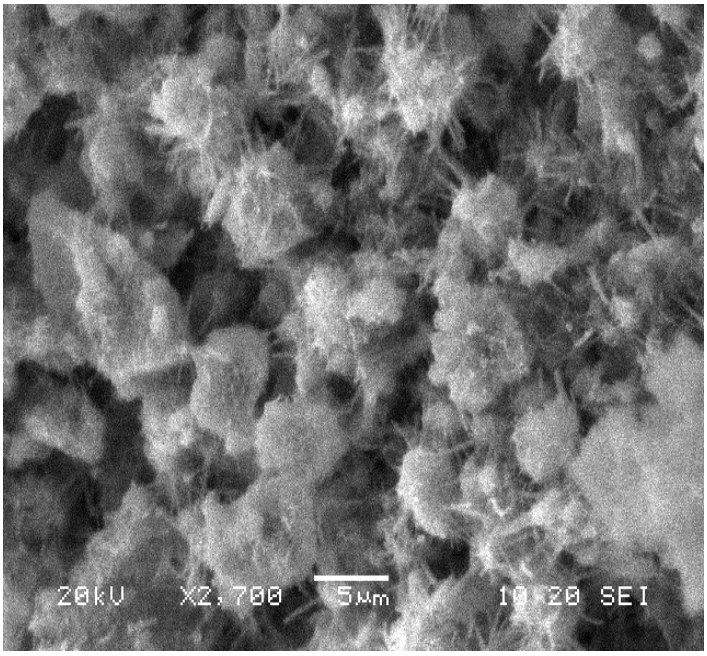

(a)

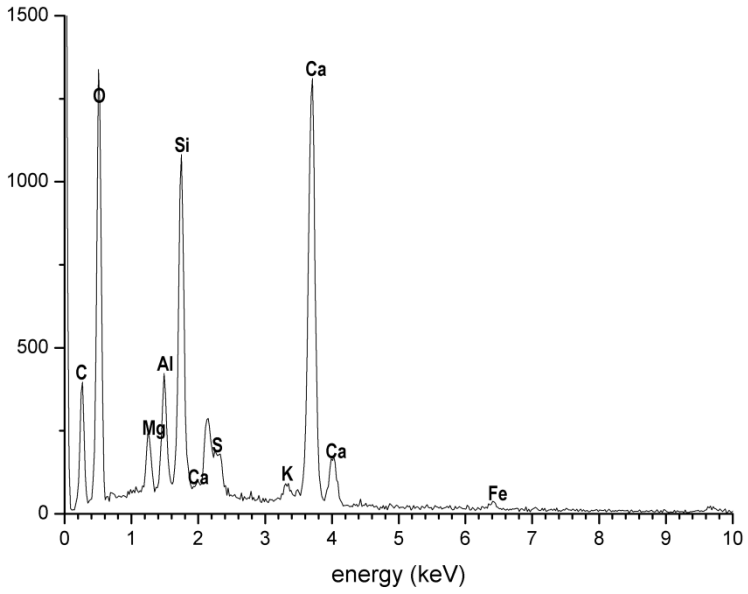

(b)

Fig 10: SEM image of mortar samples, 56 days age after the pre-cracking phase and the first 28 days healing curing period (a); EDS analysis: the sample was sputter coated with gold, whose peaks are visible in the spectrum but not labeled because they do not belong to the sample (b)

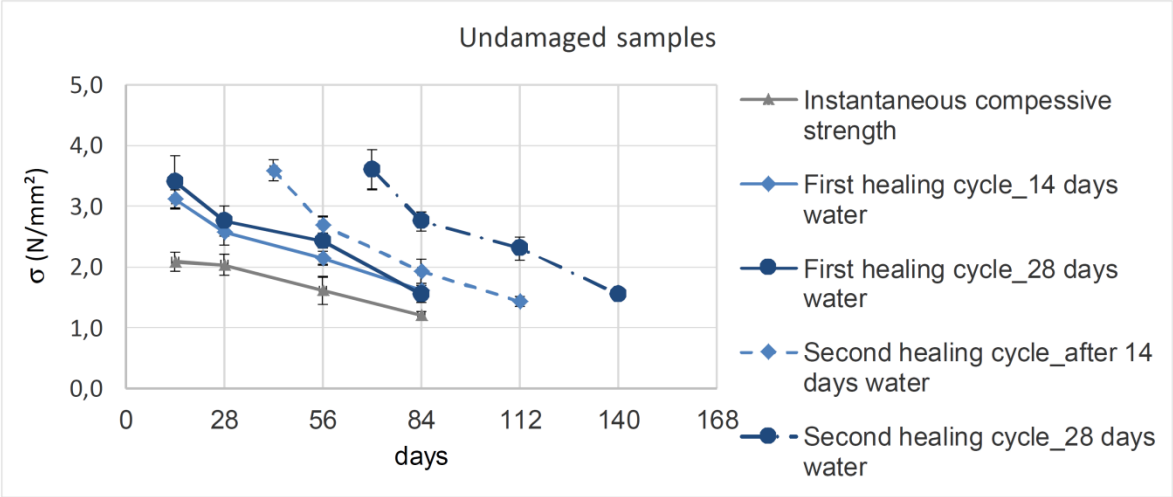

(a)

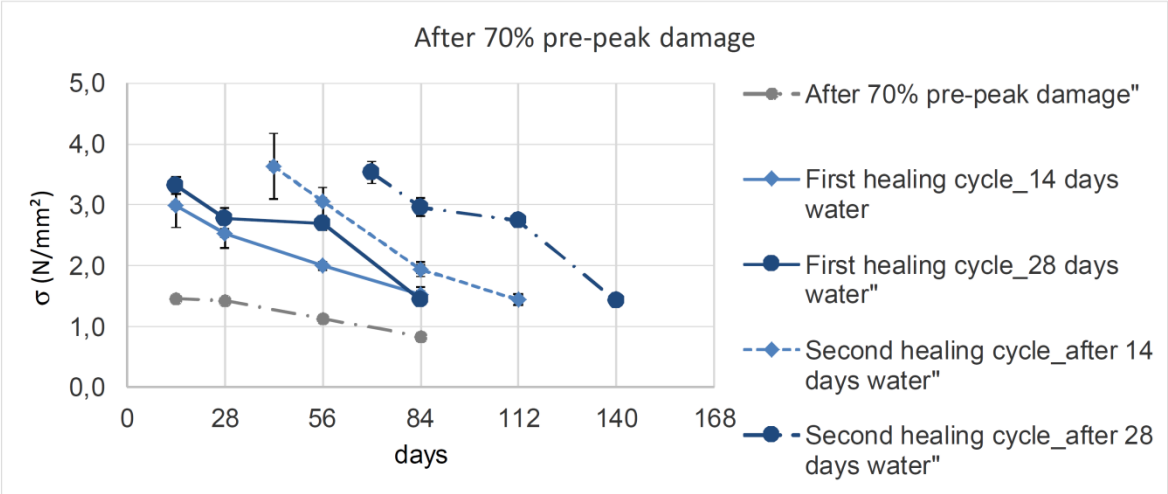

(b)

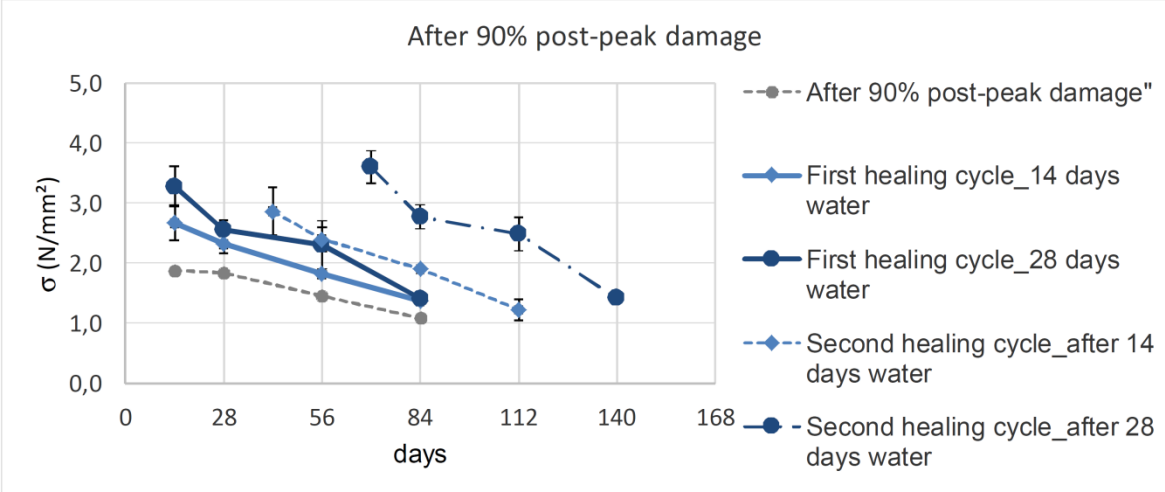

(c)

Fig 11: variation in compressive strength after pre-damage, first healing, second healing. Undamaged samples (a); samples after pre-peak regime damage; samples after post-peak regime damage (c)

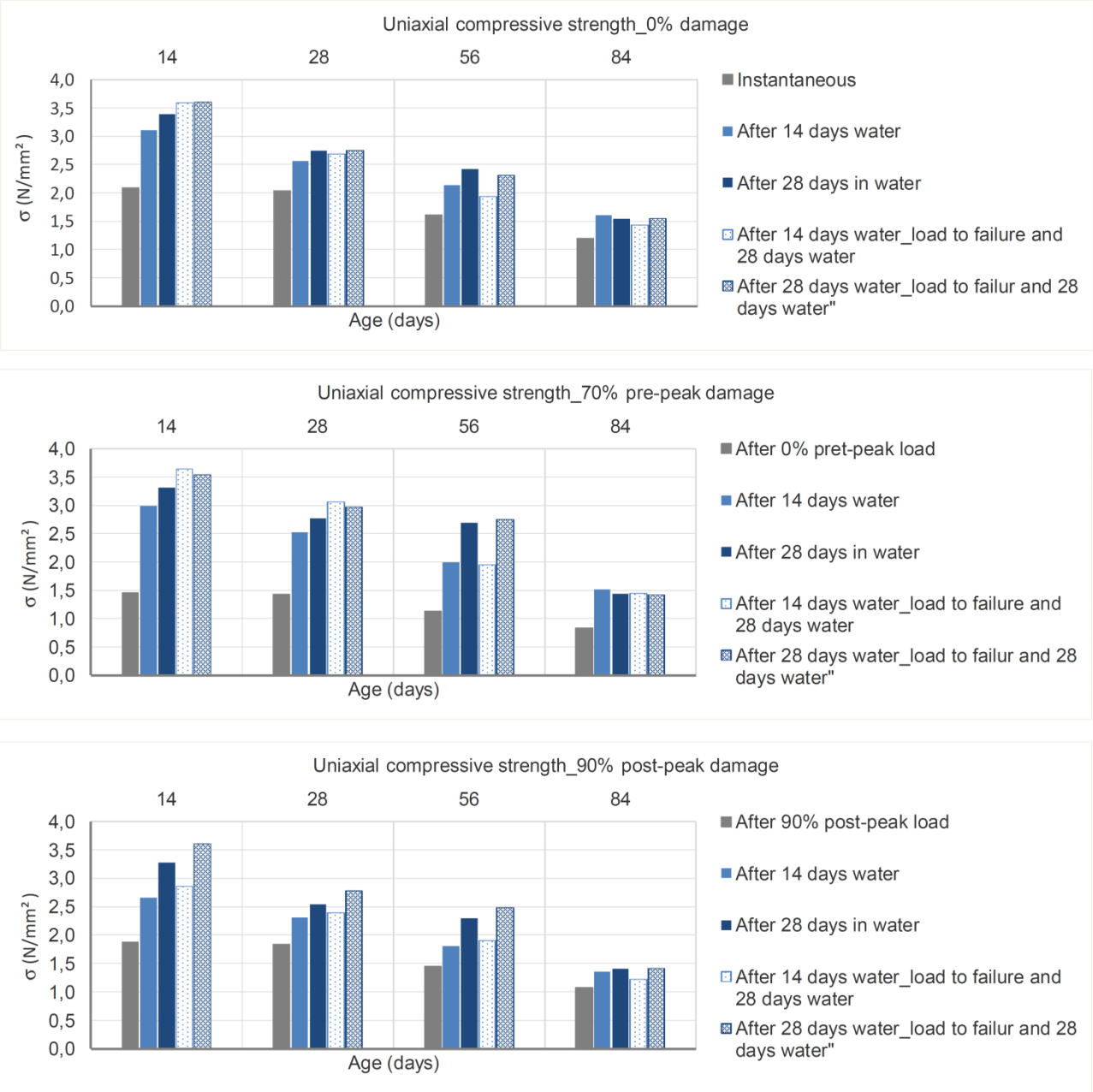

Fig 12: recovery of compressive strength after first healing cycle and second healing cycle.